

Palynofacies classification of submarine fan depositional environments: outcrop examples from the Marnoso-Arenacea Formation, Italy

McArthur A.D.¹, Gamberi F.², Kneller B.C.³, Wakefield M.I.⁴, Souza P.A.¹ & Kuchle J.¹

1. Instituto de Geociências, Universidade Federal do Rio Grande do Sul, Porto Alegre, RS 91501-970, Brazil

2. Istituto di Scienze Marine, ISMAR-CNR, Via Gobetti 101, 40129, Bologna, Italy

3. Department of Geology & Petroleum Geology, University of Aberdeen, Aberdeen, AB24 3UE, UK

4. BG Group, Geoscience Studies team, Exploration Department, 100 Thames Valley Park Drive, RG6 1PT

Abstract

Basin floor fans contain some of the largest deep-water hydrocarbon accumulations discovered, however they also demonstrate extremely complex stratigraphic architecture, understanding of which is crucial for maximum recovery. Here we develop a new method, based upon palynofacies analysis, for the distinction of the different depositional environments that are commonly associated with basin floor fans. Previous studies and our sedimentological analysis allow good confidence in the discrimination of the different depositional environments of the outcropping Marnoso-Arenacea Formation fan system. One hundred and thirty-five samples were collected from mudstones in conjunction with sedimentary logging of 871 m of outcrops. Six lithofacies associations are described and interpreted to represent lobe axis, lobe fringe, fan fringe, contained interlobe, basin plain, and starved highs. Palynofacies of these elements demonstrate turbidites to be rich in terrestrial organic matter, with sixteen categories of matter recognised. The abundances and proportions of particles varies between sub-environments, with lobe axis deposits containing the largest, densest particles, with a transition to ever smaller and lighter particles moving toward the basin plain. Fuzzy C-means statistical analysis was used to explore this trend. Distribution of organic matter is not random, but is dominated by hydrodynamic sorting and sequential fall-out of particles as turbidity currents passed across the basin. This allows a palynofacies classification scheme to be constructed to assist the identification of depositional environments of submarine fans, which may be combined with subsurface data to assist reservoir characterisation.

Keywords: deep-marine, particulate organic matter, turbidites, outcrop analogue, reservoir architecture, Miocene

1. Introduction

Basin floor submarine fans are sites of some of the largest deep-water hydrocarbon fields discovered, e.g. the Forties Field, North Sea (Rose et al., 2011); Mad Dog, Gulf of Mexico (Oyedele et al., 2015); Leviathan, Eastern Mediterranean (Lazar et al., 2012), and they remain important exploration targets across the globe. Basin floor fans are typically large and complex systems and the understanding of their detailed architecture is essential for maximising and maintaining production (Hempton et al., 2005). Single depositional elements may be difficult to distinguish purely with geophysical, petrophysical, or even core data, and often extensive outcrop analogues are employed (e.g. Wickens and Bouma, 2000; Browne and Slatt, 2002; Hubbard et al., 2005; Prelat et al., 2009; Barton et al., 2010; Jobe et al., 2010; Alpak et al., 2013). As such, any tool that may be used to enhance our understanding of the distribution of reservoir and non-reservoir facies must be seen as an advantage for the planning of exploration and development strategies.

One such tool is the application of palynofacies classification schemes to submarine fan deposits. Palynofacies is the study of all acid-resistant, microscopic particulate organic matter contained within sediments (Combaz, 1964) and recent studies of deep-water turbidite systems have shown them to be rich in a variety of organic matter (Beaudouin et al., 2004; Baudin et al., 2010; Biscara et al., 2011; Stetten et al., 2015; McArthur et al., 2016a). Organic particles behave as any sedimentary particle when entrained by currents (Muller, 1959; Stanley, 1986), and we hypothesize that their distribution is not random in turbidite systems, but is largely controlled by transport processes, which gives hints regarding the environment of deposition.

This paper represents the third piece of a new classification scheme for turbidites, complementing recent companion works establishing palynofacies classification schemes for slope channels (McArthur et al., 2016a) and mini-basin confined turbidites (McArthur et al., 2016b). A natural laboratory, with good confidence in the depositional environment was required to test our hypothesis. As such, well-studied, world-class outcrops were logged and sampled, using outcrops of the Marnoso-Arenacea Formation, in the Apennine fold and thrust belt of northern Italy (Fig. 1). These outcrops provide an excellent stratigraphic framework, with extensive studies being conducted over the last fifty years (see Ricci Lucchi, 1978; Ricci Lucchi and Valmori, 1980; Ricci Lucchi, 1986; Mutti et al., 2002; Amy and Talling, 2006; Muzzi Magalhaes and Tinterri, 2010; Tinterri and Muzzi Magalhaes, 2011; Talling et al., 2012; Talling et al., 2013; Malgesini et al., 2015; Tinterri and Tagliaferri, 2015; Tinterri et al., 2016, and references therein).

This study aims to 1) document reservoir scale depositional environments of a basin floor submarine fan; 2) examine the type of particulate organic matter delivered to and preserved in these depositional elements; 3) develop a palynofacies classification scheme to assist the interpretation of sub-environments in deep-water settings. This study does not seek to replicate bed-for-bed scale correlations already produced by Muzzi Magalhaes and Tinterri (2010) and Tinterri and Tagliaferri (2015) amongst others, instead key sections representative of selected depositional environments were studied and sampled in order to investigate their palynofacies. The definitive goal is to provide a classification scheme applicable to sub-surface studies, to aid characterisation of sub-surface submarine fans, understanding of which is crucial for hydrocarbon exploration and development.

2. Geological setting

The Miocene Marnoso-Arenacea Formation preserves a down-dip transect of a submarine fan system, extending over 200 km from north to south along the northern Apennines (Fig. 1a) and exhibits over 3500 m of stratigraphy (Ricci Lucchi and Valmori, 1980; Gandolfi et al., 1983; Ricci Lucchi, 1995; Roveri et al., 2002; Muzzi Magalhaes and Tinterri, 2010). Deposition occurred in a NW-SE orientated, elongate foreland basin of the Proto-Adriatic, which developed to the east of the Apennine thrust belt (Ricci Lucchi, 1965; Ricci Lucchi, 1967; Ricci Lucchi, 1969; Ricci Lucchi, 1975a; Ricci Lucchi, 1975b; Ricci Lucchi, 1978; Gandolfi et al., 1983; Ricci Lucchi, 1983; Argnani and Ricci Lucchi, 2001; di Biase and Mutti, 2002; Roveri et al., 2002; Lucente, 2004). Sediments were primarily sourced from fluvio-deltaic systems of the Alpine chain to the north, forming turbidity currents running SE as axial flows, with subsidiary calcareous flows termed “Colombine” by Ricci Lucchi and Valmori (1980), which were sourced from carbonate platforms in the south, and mass-transport complexes (MTCs) locally derived from the propagating Apennine thrust front (Ricci Lucchi, 1975b; Ricci Lucchi, 1978; Gandolfi et al., 1983; Ricci Lucchi, 1983; Ricci Lucchi, 1986; Lucente, 2004; Amy and Talling, 2006; Lucente and Pini, 2008).

Deposition in the basin has been broadly divided into two gross units. The older (Burdigalian to Serravallian) unconfined to poorly confined stage, is termed the “inner” basin (Ricci Lucchi, 1983). Although still much debated, thrusts may have been active in the Burdegalian to lower Serravallian (Tinterri and Muzzi Magalhaes, 2011), but individual flows may be traced over 120 km and a wide (>60 km) and low gradient basin plain is envisaged (Ricci Lucchi and Valmori, 1980; di Base and Mutti, 2002; Amy and Talling, 2006). Increasing tectonic confinement is inferred from progressive segmentation and narrowing of the basin in the upper Serravallian (Tinterri and Tagliaferri, 2015), leading to the deposition of lobe systems (Tagliaferri and Tinterri, 2016). Subsequent Tortonian age deposits form the “outer” basin stage (Ricci Lucchi, 1983), coinciding with a basin compartmentalisation due to

syndepositional structural high growth, leading to channelised turbidite systems (Ricci Lucchi, 1983). As development of the Apennines continued, a progressive shallowing of the basin occurred into the Messinian, ultimately leading to closure of the basin (Mutti et al., 2002). Subsequently the basin has been deformed and segmented by ongoing thrusting and uplift to form the studied outcrops (Roveri et al., 2002).

Deposition of the studied interval occurred above the Contessa marker bed, during the Serravallian “inner stage” (Fig. 1b; Amy and Talling, 2006; Talling et al., 2007; Muzzi Magalhaes and Tinterri, 2010; Tinterri and Muzzi Magalhaes, 2011; Sumner et al., 2012; Talling et al., 2012; Tinterri and Tagliaferri, 2015). The studied deposits are concentrated in the Santerno to Bidente depocentre, which is separated from a southern depocentre by the Verghereto High (Fig. 1a; Ricci Lucchi and Valmori, 1980; Amy and Talling, 2006).

Excellent field mapping by the Italian Geological Surveys has allowed key marker beds to be traced across the study area and gives confidence in correlation between outcrops. This permits components of submarine fans, including lobes to be subdivided into their various depositional elements.

3. Methodology

3.1 Sampled intervals

This study considered Units II-V of the Marnoso-Arenacea Formation described in detail by Muzzi Magalhaes and Tinterri (2010). However, not all of their lithofacies and elements were studied, instead focusing on the primary turbiditic components of basin floor fans. Mass-transport deposits were not investigated as they provide information regarding the remobilized material rather than the final environment of deposition. Seven sections were logged at 1:50 scale, totalling 871 m thickness to allow recognition of lithofacies, lithofacies associations

consisting of groupings of related lithofacies, which can be interpreted to represent depositional environments. Studied sections comprised:

- A lower Serravallian interval of Units III and IV of Muzzi Magalhaes and Tinterri (2010), above the Contessa marker bed (Fig. 1b), describing a relatively proximal section at Coniale, in the Santerno Valley, an intermediate section comprising the lower portion of the Sambuca Road (Fig. 1a) and a more distal equivalent at Cabelli in the Bidente Valley (Fig. 1a).
- The upper Serravallian Unit IV of Muzzi Magalhaes and Tinterri (2010) interval between the Susinello and Casaglia MTCs (Fig. 1b), including one proximal section located on the Sambuca Road, and one distal section in the Mandrioli Pass (Fig. 1a).
- The upper Serravallian Unit V of Muzzi Magalhaes and Tinterri (2010) sections located above the Casaglia MTC (Fig. 1b), being a proximal section near Firenzuola, the upper part of the Sambuca Road and a relatively more distal equivalent in the Civitella di Romagna area (Fig. 1a).
- The marls of the Verghereto region (Fig. 1a), which are correlative with Unit V of Muzzi Magalhaes and Tinterri (2010).

3.2 Palynological processing

One hundred and thirty-five samples, each 10 g, were collected in conjunction with sedimentary logging of sections. Samples were impartially taken at regular intervals (minimum of 5 m) from clean, fresh outcrop, and were taken from mudstone to avoid a lithological influence on the organic matter. Samples were primarily taken from the turbidite component of mudstones, except in locations where this was not present and hemipelagic mudstone was instead collected. The sampling strategy was planned to assess both lateral and vertical variations in palynofacies, by means of sampling correlated sections.

A standard processing technique (Table 1) was used to avoid variations in matter recovery. A minimum of three hundred pieces of particulate organic matter were counted per slide, using a Leica DM2500 binocular biological microscope, with differential interference contrast, and fluorescent light. The minimum, maximum and average size of phytoclasts (microscopic plant fragments) were recorded; along with their degree of rounding and sphericity; the dominant morphological features of miospores and dinoflagellate cysts; level (high, moderate, low) and types (bacterial degradation, chemical corrosion, mechanical damage, mineralisation) of deterioration shown by particles. The long axis length of the first forty equant opaque phytoclasts observed was recorded for each sample.

Particulate organic matter was categorised by its transmitted and fluorescent light properties (Fig. 2), with sixteen groups of material recognised. Categories are based upon the observed particles, but agree with those of McArthur et al. (2016a) and McArthur et al. (2016b) thereby providing a uniform scheme, applicable across a wide range of deep-marine sub-environments. Groupings may be separated into allochthonous terrestrial material, interpreted to have been transported a reasonably long distance and relatively autochthonous marine debris (Fig. 2). Groupings are sorted by their inferred density as described by Muller (1959), Cross et al. (1966), Traverse and Ginsburg (1967), Chaloner and Muir (1968), Riley (1970), Davey (1971), Koreneva (1971), Davey and Rogers (1975), Batten (1982), Tyson (1984), Kohl (1985), Boulter and Riddick (1986), van der Zwan (1990), Whitaker et al. (1992), Tyson (1995), Hoorn (1997), Oboh-Ikuenobe et al. (1999), Beaudouin et al. (2004), Jäger and McLean (2008) and Baudin et al. (2010). Fungal material was not subdivided (*sensu* Boulter and Riddick, 1986), and well-preserved wood and parenchyma were also grouped (*sensu* van der Zwan, 1990). All slides, residues, and samples are housed in the Marleni Marques Toigo Laboratory of Palynology at UFRGS, Porto Alegre, Brazil.

3.3 Statistical analysis

Fuzzy C-means (FCM) cluster analysis is a data investigation and classification tool, which identifies entities, in this case samples, with similar compositions. Termed fuzzy due to fact that samples can have an association with multiple clusters, as opposed to hard clustering techniques such as correspondence analysis, making FCM ideal for datasets with high degrees of similarity between samples (Gary et al., 2009). This is important for large, gradational palaeontological datasets, which often include samples that are transitional between hard clusters (Gary et al., 2009; Daly et al., 2011; Erbs-Hansen et al., 2011, 2012; Churchill et al., 2016; McArthur et al., 2016b). This methodology is particularly appropriate for the Marnoso-Arenacea dataset, which aims to examine the changes in sedimentation from turbidity currents that graded across an area in excess of 3600 km² (Fig. 1; Muzzi Magalhaes and Tinterri, 2010). Therefore this method was chosen over relatively more simple hard clustering techniques.

FCM was performed using the Technical Alliance for Computational Stratigraphy (TACSworks) software. FCM is an investigative technique used to identify clusters of samples with related configurations (Zadeh, 1965). Each data point (sample) may belong to any cluster, permitting representation of samples that are gradational between multiple clusters (Gary et al., 2009). Conditioning the FCM model is an iterative process, with the one disadvantage of FCM over hard clustering methods being the time required to condition the dataset and identify the correct number of clusters. We followed the process espoused in Gary and others (2009) and illustrated in Churchill and others (2016).

The fuzzy exponent was varied between a hard cluster (1.1), which is close to traditional clustering techniques, and a soft cluster (3.0), where memberships to clusters tend to be highly gradational, in order to better understand the data structure and provide a guide to constraining the FCM parameters. Two criteria are used to judge the best amount of clusters, being compaction and separation (Gary et al., 2009). Compaction refers to sample density around each of the cluster centres, with compact clusters being preferred, as samples associated with

a cluster will be well represented by the characteristic biota. Separation is a measure of the degree of uniqueness of the cluster centres; cluster centres that are too close will be difficult to separate, therefore some cluster separation is preferred although the clusters will in most likelihood overlap given most depositional and environmental systems display a degree of gradation. This is the main benefit of using the FCM approach.

Seven clusters were identified as the optimum solution, using an optimal fuzzy exponent value of 1.5. If more clusters were defined then model integrity was lost as similarity was too high; less clusters reduced the ability to investigate the dataset as the similarity between clusters was too high. Each defined cluster is characterised by their dominant component (organic matter type), which is identified by the cluster centroids (Table 2). The membership of each sample to each cluster is expressed from 0 to 1, where 0 is no relation and 1 is the same. The output is the percentage to which each sample belongs to each cluster, which can then be used to examine sets of samples with similar properties. See Gary and others (2009) for a detailed explanation of the FCM methodology.

4. Sedimentology

Many sedimentological studies of the Marnoso-Arenacea Formation have been conducted over the previous fifty years (see Muzzi Magalhaes and Tinterri, 2010 and references within; Tinterri and Muzzi Magalhaes, 2011; Sumner et al., 2012; Talling et al., 2012; Dall'Olio et al., 2013; Talling et al., 2013; Amy et al., 2015; Malgesini et al., 2015; Tinterri and Tagliaferri, 2015; Felletti et al., 2016; Tagliaferri and Tinterri, 2016). This allowed high resolution logging and sampling to be carried out to identify key depositional environments represented in the Marnoso-Arenacea Formation. Although workers such as Amy and Talling (2006) and Muzzi Magalhaes and Tinterri (2010) recognised a wider range of deposits, the focus of this study was the turbidites.

4.1 Depositional environments

By grouping lithofacies, observations of their occurrences and relationships allow us to define specific depositional sub-environments of the system. Each element shows subtle variations across the basin, such as the dominant grain size, degree of bed amalgamation, thickness of mud-caps, and net to gross (N:G). These and other factors have been used by previous workers to subdivide the siliciclastic stratigraphy into relatively proximal to distal settings from NW to SE (Ricci Lucchi, 1975a; Ricci Lucchi and Valmori, 1980; Ricci Lucchi, 1985; Mutti et al., 2003). Work by Muzzi Magalhaes and Tinterri (2010), Tinterri and Muzzi Magalhaes (2011), Tinterri and Tagliaferri (2015), Tagliaferri and Tinterri (2016) and Tinterri and others (2016) have also recognised the influence of growth structures on the stratigraphy, which also influenced the distribution of sub-environments in the upper Serravalian stage of the basin fill.

4.1.1 Depositional environment A – Lobe axis (Fig. 3)

Observations: Thick-bedded turbidites (>80 cm), dominantly comprised of laterally continuous sandstones occurring in sheet-like beds (lithofacies F8 of Mutti et al., 2003), often amalgamated into packages meters to tens of meters thick (Fig. 3). Amalgamations of beds are marked by subtle grain size breaks or mud-clast rich horizons, and this element shows the highest N:G of those studied here. When present, finer grained caps (lithofacies F9 of Mutti et al., 2003) may be up to 50 cm thick, and consist of silty cross-laminations (Fig. 3), often with a concentration of plant debris. Bioturbation is common including large burrows such as *Ophiomorpha*. Sole marks are directed towards SE (Tagliaferri and Tinterri, 2016). The northern, more proximal areas of the basin, e.g. Firenzuola, commonly show the highest N:G and degree of bed amalgamations, dominantly coarse to medium grain size, a high proportion of beds with scoured bases and mudstone clasts (Fig. 3) and finer grained caps up to 15 cm

thick. The central portions of the basin, e.g. Sambuca, commonly show beds with an upper, finer-grained sand- to siltstone portion (lithofacies F9 of Mutti et al., 2003) up to 50 cm thick, having a marginally lower N:G (c. 90%), and are dominantly medium to fine-grained. Although scours are present they are shallower than in northern sections and mud-clast intervals are rare. This element was not observed in southern area of the basin.

Interpretation: Lobe axis - This association of thick-bedded, sheet-like, laterally continuous turbidites, mainly consisting of sandstones are interpreted as the deposits of high (Bouma Ta) and low density (Bouma Tbc) turbidity currents, representing lobe axis deposits. These deposits correspond to Unit V described by Muzzi Magalhaes and Tinterri (2010) and are dominated by Type 4 beds of Muzzi Magalhaes and Tinterri (2010), which they interpreted as normal graded beds deposited from waning and depletive flows. In the northern Firenzuola area the coarse grain size, degree of scour, and bed amalgamations implies these represent the relatively proximal portion (Ricci Lucchi, 1975a), which may have been preferentially ponding in bathymetric lows (Tinterri and Tagliaferri, 2015). Lack of, or very thin, fine-grained caps imply upper portions of flows were bypassing to more distal parts of the basin or were removed by erosional processes due to subsequent flows, the former explanation being favoured by Tinterri and Tagliaferri (2015) and used to illustrate flow stripping by confinement. Moving SE to the Sambuca area (Fig. 1), a reduction in average grain size, relatively thinner scour depths, and a reduced degree of bed amalgamation imply transition to the intermediate portion of the basin (Ricci Lucchi, 1975a; Ricci Lucchi and Valmori, 1980).

4.1.2 Depositional environment B – Lobe fringe (Fig. 3)

Observations: Dominantly graded, and structured turbidite beds with medium to thin-bedded basal sandstones (lithofacies F8 to F9 of Mutti et al., 2003) capped by turbidite mudstone in packages up to 10 m thick (Fig. 3). Showing a relatively high N:G, being up to

70% sandstone in graded beds up to 1 m thick, with typically subordinate mudstone cap division no more than 20 cm thick (Fig. 3). Thicker (>1 m) sandstones (lithofacies F8 of Mutti et al., 2003) are rarely interbedded (Fig. 3). Beds have a laterally extensive sheet-like distribution over hundreds of meters, with sharp, flat basal contacts. Loading of sandstone into underlying mudstones is common. Mud-clast debrites occur very rarely in this element. Bioturbation is pervasive throughout the sand- and mudstones, but not in the debrites. These deposits typically grade up from thick-beds of the lobe axis (Fig. 3). This element is typically thickest in central portions of the basin (e.g. Sambuca), where it has a moderate N:G, graded sandstone to mudstone beds thinner than 75 cm, and thick sandstones are rare. In the northern portions (e.g. Firenzuola), beds are typically thicker and F8 type beds are more commonly intercalated. These packages are also present in the southern areas of the basin (e.g. Civitella), where N:G is lower, with mudstone caps representing up to 50% of the beds; and thicker F8 type sandstones are very rare.

Interpretation: Lobe fringe - These dominantly medium- to thin-bedded turbidite sandstones, capped by variable amount of turbidite mudstone, with occasional thick-bedded sandstones, which typically grade up from thicker lobe axis deposits are interpreted as the deposits from low density turbidity currents (Bouma Tbe) on a lobe fringe (sensu Prelat et al., 2009). As with the associated thick-beds of the lobe axis, these deposits are contained within Unit V of Muzzi Magalhaes and Tinterri (2010). Given these deposits grade from the lobe axis deposits, they should not be confused with the reflected beds of Muzzi Magalhaes and Tinterri (2010), but represent a sub-division of their lobes. Although often disrupted by bioturbation, the structures and range of grain sizes within the mudstone intervals implies the mud-caps were primarily deposited from turbidity currents. The mud clast debrites are interpreted to represent hybrid event beds (sensu Haughton et al., 2003). The reduction in N:G, decreasing abundance of thick-beds, and increasing proportion of thin-bedded turbidites from NW to SE indicates a

transition from proximal to distal portions of the basin (Ricci Lucchi, 1975a; Ricci Lucchi and Valmori, 1980).

4.1.3 Depositional environment C – Fan fringe (Fig. 4)

Observations: Graded turbidite beds 20-100 cm thick (Lithofacies F9 of Mutti, 2003) and hemipelagic mudstones, give rise to mudstone dominated successions (N:G <30%), meters to tens of meters thick (Fig. 4). Sandstones are typically <20 cm thick and show extensive traction structures before grading into mudstones. These packages are laterally extensive over hundreds of meters across any one outcrop. Sandstones may show dewatering and loading into underlying mudstones. Turbidite mudstone caps are typically dark grey and laminated, but often grade into a pale-grey, massive, calcareous, upper component (Fig. 4). Rarely, mud clast-debrites up to 1 m thick were encountered, with clasts up to 1 m long. Bioturbation is common in sandstones and mudstones but not in the debrites. This association is present in northern (e.g. Coniale) and central portions of the basin (e.g. Sambuca). However, it is most prevalent in southern sections (e.g. Cabelli), where the mud-caps are thicker and contain higher proportions of hemipelagic mudstone when compared to central sections, where N:G is higher and the proportion of hemipelagites is lower (Ricci Lucchi and Valmori, 1980).

Interpretation: Fan Fringe - These mudstone dominated packages, with abundant hemipelagic mudstone and turbidites with basal medium to thin-bedded sandstones and rare debrites, are interpreted as fan fringe deposits (sensu Bouma and Rozman, 2000). Sandstones and laminated mudstones are interpreted to have been deposited from low density turbidity currents (Bouma Tbe), whilst light grey mudstones are hemipelagites (Talling, 2001). The studied deposits span Units III-IV of Muzzi Magalhaes and Tinterri (2010), which they note has a high proportion of hybrid event beds, as well as the thin-bedded turbidites, which is in keeping with the interpretation of a fan fringe (Kane et al., 2017). Correlations presented by

Muzzi Magalhaes and Tinterri (2010) demonstrate that the passage from thick- into thin-beds occurs through a progressive thinning and fining of the beds. Mud-clast rich beds are interpreted as hybrid event bed deposits (sensu Haughton et al., 2003). Mud-clasts tend to show a massive structure and light grey colour, similar to in-situ hemipelagic mudstone.

4.1.4 Depositional environment D – Contained interlobes (Fig. 5)

Observations: Comprising turbidites with basal thin-bedded sandstones capped by silt- and mudstones, typically more than twice as thick as the underlying sandstone, occurring in packages meters thick. The N:G is very low (<10%). Basal sandstones show traction structures such as ripples, or may occur as starved ripples. Mudstone caps are always dark grey and may show remnants of lamination (Fig. 5); however bioturbation is intensive and typically destroys sedimentary structures. These deposits are associated with the lobe deposits (Fig. 5), being most common in the northern (e.g. Firenzuola) and central (e.g. Sambuca) portions of the basin. Here they can be observed to grade out from dominantly medium bedded, sandstone rich lobe fringe deposits and are commonly terminated by overlying thicker bedded deposits (Fig. 5). They do not show significant variation in thickness or structures across the basin.

Interpretation: Contained interlobes - These turbidite mudstone dominated intervals are interpreted the result of containment of turbidity current suspensions clouds (sensu Patacci et al., 2015), during periods of low sediment supply to the basin. I.e. these are the deposits between successive lobes (sensu Mulder and Etienne, 2010), when only dilute turbidity currents were being supplied to the basin. Being associated with the Unit V lobes of Muzzi Magalhaes and Tinterri (2010), they are inferred to have been deposited during increasing confinement of the basin. That they grade from and are truncated by thicker beds of the lobe axis and lobe fringe, indicates they were deposited in the same subtle bathymetric lows as the sand-rich lobe elements (Tagliaferri and Tinterri, 2016). Care must be taken to differentiate

these deposits from fan fringe and basin plain type deposits, which contain hemipelagic mudstones.

4.1.5 Depositional environment E – Basin plain (Fig. 6)

Observations: Hemipelagic mudstone dominated packages tens to hundreds of meters thick (Fig. 6). Turbidite beds intercalated with the hemipelagic mudstone consist mainly of lithofacies F9 of Mutti (2003). Beds are laterally continuous and may be traced across outcrops over hundreds of meters, but N:G is typically <10%. Turbidite beds are typically graded, sometimes initiating with a thin (<10 cm) sandstone or more commonly a very thin (<3 cm), very fine-grained sandstone or siltstone, grading to laminated turbidite mudstone and massive hemipelagic mudstone. The sand- to siltstone component may show traction structures such as ripples or cross-lamination (Fig. 6). Tinterri and Muzzi Magalhaes (2011) note that many of the thin turbidites show combined flow structures, such as biconvex ripples with sigmoidal-cross laminae and small-scale hummocky-type structures. Rarely, isolated thicker sandstones (F8 of Mutti, 2003), mud-clast debrites, and argillaceous sandstones occur (Fig. 6), but represent <12% of this depositional environment. Bioturbation is widespread but low intensity. This element is present in central portions of the basin (e.g. Sambuca), in packages <10 m thick, but becomes the prevalent deposit in the southern areas of the basin, for example in the Mandrioli Pass (Fig. 1). The Mandrioli section is almost one kilometre thick, where hemipelagic mudstone commonly represents >50% (Fig. 6).

Interpretation: Basin plain – This association of mudstone dominated heterolithics, hundreds of meters in thickness is interpreted to represent background sedimentation on the basin plain (Ricci Lucchi, 1975a). Alternatively Muzzi Magalhaes and Tinterri (2010) proposed these style of deposits to represent sedimentation in close proximity to confining structures, but still on the basin plain. Either way, the intervals are dominated by hemipelagic

sediments, which denote large time periods, when compared to the near instantaneous turbidite deposits. Thin-bedded turbidites represent sporadic run-outs of turbidity currents that were likely depositing the majority of their load in the primary depocentre of the basin (Tinterri and Muzzi Magalhaes, 2011). The rare, isolated thicker sandstone beds represent less frequent large events, which were able to spread out and deposit across the whole of the basin (Ricci Lucchi, 1978; Ricci Lucchi and Valmori, 1980; Amy and Talling, 2006; Talling et al., 2007; Sumner et al., 2012), which may relate to pulsating combined waning flows (Muzzi Magalhaes and Tinterri, 2010). The thin, argillaceous sandstones, which may or may not show mud clasts deposits are associated with the turbidites, corresponding to tripartite beds of Muzzi Magalhaes and Tinterri (2010). The sediments in question are found in Units III-IV of Muzzi Magalhaes and Tinterri (2010) and demonstrate contained and reflected beds. The distribution of the enigmatic tripartite and relected beds is not the focus of this study, with samples being collected from the Mutti (2003) F9 type turbidites of this interval.

4.1.6 Depositional environment F – Starved high (Fig. 7)

Observations: Mudstone dominated successions tens of meters thick (Fig. 7). Rare, thin sandstones (<5 cm) grading to siltstones and turbidite mudstones up to 20 cm thick are present, but these intervals are dominated (>90%) by hemipelagic mudstones, having the lowest N:G of the described elements. Deformation of these deposits in the form of slumps and slide scars are evident. Bioturbation is commonly intensive and may destroy any primary depositional structures. This element typically sits above MTCs or areas inferred to have been intra-basinal highs during deposition, e.g. Verghereto (Ricci Lucchi and Valmori, 1980; Amy and Talling, 2006; Tinterri and Tagliaferri, 2015).

Interpretation: Starved highs – These hemipelagic dominated successions, with the lowest observed N:G of any element and an association with areas inferred to have been

bathymetric highs that were starved of sediment supply (Amy and Talling, 2006). These sections coincide with Unit V of Muzzi Magalhaes and Tinterri (2010), when it is inferred that growth structures had resulted in development of the bathymetric highs, with only thin and dilute turbidity currents able to surmount the highs. Slumps and slides indicate deposition on a slope, with periodic failure of the fresh sediment.

5. Palynofacies of basin floor fans

5.1. Palynofacies

In general, palynofacies of the Marnoso-Arenacea Formation are dominated by palynowafers (Fig. 2). However, fifteen other categories of organic matter were encountered (Fig. 2). The proportion of palynowafers to the other particles, their relative ratios, and the dimensions of particles can be used to characterise the depositional environment based upon their palynofacies associations. Data is displayed both in its raw format to view stratigraphic trends (Fig. 8), but also as box and whisker charts, demonstrating the proportions of particulate organic matter for each depositional environment (Fig. 9).

5.1.1. Depositional environment A, Lobe axis (Fig. 10A and B)

Samples taken from the axis of lobes demonstrate moderately poorly-sorted assemblages, typically with at least half the sample being comprised of large fragments (up to 300 μm) of palynowafers (Fig. 8 and 9). Lesser occurrences of degraded brown wood and amorphous organic matter (AOM) are the other main constituents (Fig. 8 and 9). Miospores show a relatively high diversity, including large rugose forms and smaller simple forms; spores may show mechanical damage and are normally at least partially pyritized. Dinoflagellate cysts were very rarely observed and have a low diversity; cysts often display mechanical damage inferred to have occurred during transport and are also usually pyritized. Samples may be

subdivided into those collected in the proximal, northern sections (e.g. Firenzuola) and the intermediate, central sections (e.g. Sambuca) (Fig. 8 and 9). This demonstrates a down-fan reduction in the proportion of degraded and well-preserved wood, with increases in palynowafers, miospores, fungi and AOM (Fig. 8 and 9). Opaque equant phytoclasts also decline moving south, with those in proximal samples up to 200 μm in diameter (Fig. 10A), whilst those in intermediate sections are less than 80 μm (Fig. 10B).

5.1.2. *Depositional environment B, Lobe fringe* (Fig. 10C - E)

Samples from the lobe fringe show moderately poorly-sorted assemblages (Fig. 8 and 9). Samples are dominated by palynowafers, AOM, and degraded wood (Fig. 8 and 9). Miospores show a relatively high diversity, including some larger forms, but are generally represented by small, simple spores, which are often pyritized. Dinocysts, although rare and pyritized show a range of both cavate and proximate forms. Three trends are apparent moving from proximal to distal settings (Fig. 8; 9 and 10C-E), with downstream reduction in degraded and well-preserved wood (Fig. 10C), reduced palynowafers in intermediate samples (Fig. 8 and 9) and AOM being most abundant in intermediate samples (Fig. 10D). Equant particles are generally smaller than in the lobe axis, reaching a maximum of 100 μm and no more than 25 μm in distal samples.

5.1.3. *Depositional environment C, Fan fringe* (Fig. 10F - H)

Fan fringe samples demonstrate the most poorly-sorted palynofacies assemblages (Fig. 8 and 9). Although still dominated by palynowafers, they typically represent less than half of the assemblage, particularly in intermediate and distal samples (Fig. 8 and 9). This sub-environment records the highest counts of palynomorphs (Fig. 8 and 9), which show a moderate diversity; miospores are typically small, simple, round spores, whilst dinoflagellate cysts typically show cavate forms, and marine algae are normally present (Fig. 8 and 9). Samples

from the fan fringe show a downstream reduction in palynofauna, increase in well preserved wood (Fig. 10F – H), whilst AOM peaks in intermediate sections (Fig. 8). Particle size is notably smaller than previous elements, reaching a maximum of 25 μm in proximal sections, reducing to 20 μm in intermediate sections, and 16 μm in distal samples.

5.1.4. *Depositional environment D, Contained interlobe* (Fig. 10I)

Contained interlobe samples are well-sorted, consistently have the highest counts of palynofauna and excepting hemipelagite samples, the lowest counts of degraded and well preserved wood particles (Fig. 8 and 9). They have the lowest proportion of AOM of the studied sub-environments (Fig. 9). A very low diversity of palynomorphs was observed, with miospores restricted to small, simple forms and dinocysts rarely observed. Trends are subtle, with the most apparent being a reduction in dinoflagellate cysts from proximal to distal (Fig. 8 and 9). Particle sizes are generally small (Fig. 10I), but do not show significant variation down-fan, reducing from a maximum of 23 μm in proximal sections to 18 μm in distal samples.

5.1.5. *Depositional environment E, Basin plain* (Fig. 10J)

Basin plain samples show moderate sorting (Fig. 8 and 9), being dominated by palynofauna, with lesser representation of AOM, and well-preserved wood (Fig. 10J). The abundance of well-preserved wood in this element may be related to its distal nature, with Boulter and Riddick (1986) indicating it can be retained in suspension longer than degraded wood. Palynomorph diversity is moderate, with low diversity of pollen and spores, but dinocysts show both cavate and proximate forms, and marine algae and bisaccate pollen are present in all samples. Particles are the smallest of any turbidite element, reaching a maximum of 15 μm .

5.1.6. *Depositional environment F, Starved highs*

Samples from the hemipelagic dominated starved highs show a marked contrast to those collected from turbidite mudstones in the other depositional environments, being well-sorted and dominated by AOM (Fig. 8 and 9). Samples are rich in dinoflagellate cysts, with minor phytoclasts (Fig. 8 and 9). Dinocysts show the largest diversity in types for any sub-environment, but miospores are limited to small, simple forms. The long axis of equant phytoclasts shows a maximum of 13 μm .

5.2. Statistical analysis

Given the complex, gradational nature of studied sub-environments and the inherent variability of turbidity currents passing over such a large area, statistical investigations of particle variation are required. As outlined in the methodology (section 3.3) FCM was applied (Fig. 11), being ideal for handling large and gradational biofacies datasets (Gary et al., 2009; Martin et al., 2013). All clusters are dominated by palynofauna to a varying degree (Fig. 11), but show variations in the other dominant matter types (Table 2). The fact that palynofauna dominate every element (barring the starved sections), indicates that the secondary, and tertiary constituents should be analysed to examine the dataset.

Cluster 1 shows the strongest affinity with palynofauna, with a cluster centroid value of 75.3 (Table 2) and minimal representation of any other particle type. Cluster 2 is dominated by palynofauna (cluster centroid value 62.9), with minor representation by AOM (cluster centroid value 8.8), and degraded wood (8.3). AOM dominates cluster 3 (cluster centroid value 65.0), with minor palynofauna (cluster centroid value 8.8). Cluster 4 also shows moderate representation by AOM (cluster centroid value 25.7) and degraded wood (cluster centroid value 12.7), but is most represented by palynofauna (38.6). Cluster 5 is dominated by palynofauna (cluster centroid value 52.1), AOM (cluster centroid value 15.7), and degraded wood (9.8). Cluster 6 shows the highest representation by degraded wood (cluster centroid value 20.1),

though dominated by palynofauna with a cluster centroid value of 39.1, and AOM (cluster centroid value 15.6). Cluster 7 shows the strongest relationship with well-preserved wood (cluster centroid value 7.1), but is dominated by palynofauna (59.0), and degraded wood (16.9).

Proximal lobe axis samples show the highest membership in cluster 6 and a lesser membership in cluster 7 (Fig. 11), being poorly-sorted, but rich in palynofauna and wood fragments. Intermediate lobe axis samples show most membership in clusters 4 and 2 (Fig. 11), having increased palynofauna and decreased wood compared to the proximal equivalent.

As with the lobe axis, proximal lobe fringe samples show highest membership in cluster 6, but also show membership in clusters 3 and 5 (Fig. 11), being rich in palynofauna and degraded wood. Intermediate lobe fringe samples have the highest membership in clusters 3 and 1 (Fig. 11), with increased AOM, decreased palynofauna, and less degraded wood compared to their proximal expression. Distal lobe fringe samples display highest membership in clusters 3 and 2 (Fig. 11), being almost entirely dominated by palynofauna.

Proximal fan fringe samples are dominantly represented in cluster 2 (Fig. 11), having the highest proportion of palynofauna. Intermediate fan fringe samples have highest membership in clusters 1 and 4 (Fig. 11), having amongst the lowest palynofauna of any environment and higher AOM. Distal fan fringe samples have the most membership in clusters 7 and 4 (Fig. 11), having poorly-sorted assemblages.

The proximal contained interlobe is best represented in cluster 2, but also with strong membership in clusters 4 and 5 (Fig. 11), being rich in palynofauna but with near even representation in the other matter types (Fig. 9). Intermediate contained interlobe samples are also dominated by cluster 2, with minor membership in cluster 3 (Fig. 11), also being rich in palynofauna, but with reduced AOM compared to the proximal contained interlobe. The distal

contained interlobe samples show greatest membership in clusters 2, 5, and 3. Basin plain samples show greatest membership of cluster 5 (Fig. 11) being dominated by palynofauna and lesser AOM.

6. Discussion

6.1 Distribution of particulate organic matter in basin floor fan turbidite systems

The foredeep of the Proto-Adriatic basin was clearly a marine basin, as confirmed by the presence of diverse dinoflagellate cysts and marine algae. However the abundance of terrestrially derived particulate organic matter implies significant supply of material from a nearby landmass. Provenance and palaeocurrent data indicate that the majority of the studied turbidites were sourced from multiple points along a wide shelf developed to the north of the Marnoso-Arenacea basin (Ricci Lucchi and Valmori, 1980; Gandolfi et al., 1983; Ricci Lucchi, 1983; Mutti et al., 2002; Muzzi Magalhaes and Tinterri, 2010). This is consistent with our results, which demonstrate an abundance of degraded terrestrial organic matter that may have been stored in deltaic and shelf environments, before being supplied to the deep-sea. Along continental margins, the highest concentrations of organic matter are commonly found near the shelf edge (Shepard, 1956; Muller, 1959; Uchupi and Jones, 1967; Parry et al., 1981), the area where turbidity currents triggered by sediment failure, or oceanographic processes most likely originate (Reading and Richards, 1994).

A large variety of factors have been inferred to influence the distribution and preservation of organic matter in marine environments (Zonneveld et al., 2010), with currents, local vegetation, and oxygenation being identified as the key factors (Tyson, 1995; Jäger and McLean, 2008). However, given the studied turbidites had similar source areas and levels of oxygenation are inferred to have been relatively uniform across the basin, the different behaviour of turbidity currents are implicated as the primary control on the palynofacies. It is

known that turbidity currents may entrain organic matter and carry them down-fan (e.g. Muller, 1959; Cross et al., 1966; Caratini et al., 1983; Tyson, 1984; Boulter and Riddick, 1986; Stanley, 1986; Heusser, 1988; Caratini, 1994; Tyson, 1995; Hoorn, 1997; Oboh-Ikuenobe and Yepes, 1997; Oboh-Ikuenobe et al., 1999; van der Kaars, 2001; Beaudouin et al., 2004; Hooghiemstra et al., 2006; Baudin et al., 2010; Schiøler et al., 2010; Biscara et al., 2011; Stetten et al., 2015). Turbidity currents are capable of transporting organic particles for hundreds of kilometres (Caratini, 1994), during which hydrodynamic sorting of particles occur, based upon particle size, density, shape, and texture (Fig. 2; Muller, 1959; Cross et al., 1966; Traverse and Ginsburg, 1967; Holmes, 1994). Therefore the smallest, lightest material has the greatest potential for transportation by turbidity currents and vice versa. The abundance of palynofauna observed in the studied succession is not unexpected; particulate organic matter in turbidite lobes of the modern Congo Fan are dominated by “*well-preserved translucent plant fragments*” (Stetten et al., 2015, p.186) and may be explained by the following factors:

1) Source area – Storage in a broad shelf, as proposed by Mutti (2003) before transport to the deep-sea may have led to the observed concentration of palynofauna. In addition to concentrating organic matter in the outer shelf environment, a relatively long residence time on the shelf may also explain the observed abundance of palynofauna compared to other phytoclasts, since shallow marine processes break down cuticle to fine fragments (Spicer, 1989).

2) Resistant nature of palynofauna – Cutan, the main component of plant cuticle, is considered to be highly resistant to both biological and mechanical degradation in marine environments (Staplin, 1969). The relatively uniform dark grey colour of sampled turbidite mudstones and the pervasive bioturbation observed in the sediments implies a relatively well oxidised basin plain, which may lead to increased bacterial degradation of organic matter. Cuticle is considered indigestible by bacteria and most forms of fungi (Tyson, 1995 and

references within), hence it may be preferentially preserved in oxic marine environments. Palynowafers are also more resistant to mechanical breakdown than more brittle humic phytoclasts (Neavel, 1981). This mechanical resistance may lead to relative enrichment of palynowafers over other organic particles, given potential transport in fluvio-deltaic systems, relatively long residence time in shallow marine settings, and transport of tens to hundreds of kilometres by turbidity currents (Mutti, 2003).

3) Relatively distal nature of terminal basin floor fans – Palynowafers are the most buoyant phytoclast type (Fig. 2), with their thin, platy nature retarding settling (Boulter and Riddick, 1986). This allows palynowafers to remain in suspension at low energy and to be transported into the relatively distal areas of submarine fans, where they may become concentrated relative to other types of organic particles. McArthur et al. (2016a) reported relatively proximal slope channels to be dominated by the denser types of phytoclasts, with the inference that the lighter fraction, such as palynowafers, had bypassed down slope, i.e. to basin floor fans as is evidenced by the present study.

Nonetheless, the variation in relative proportions of palynowafers and other organic particles may yield insights into the depositional sub-environments. Although dominated by terrestrial particles, each element also contains marine particles (Fig. 9). This may be due to storage on the shallow marine shelf, which commonly shows abundance of marine AOM and is also where the largest diversity of dinoflagellate cysts are to be found (Caratini, 1994). However a general enrichment of marine to terrestrial particles is seen in lobe axis to fan fringe transects (Fig. 8), which may be the result of mixing ambient seawater with the passing turbidity current, or erosion and entrainment of sea-floor sediment by passing currents.

6.2. Palynofacies classification of basin floor fans

The distribution of organic particles in the Marnoso-Arenacea Fm. reflects the various sub-environments of the submarine fan system and allows us to extend our classification scheme to help in the predictions of depositional environments within basin floor fans (Table 3; Fig. 12). Due to the nature of submarine fans, formed by repeated, essentially similar flows initiating at distance and depositing material across a wide area in a gradational pattern (Ricci Lucchi and Valmori, 1980; Ricci Lucchi, 1983; Ricci Lucchi, 1986; Mutti et al., 2003; Prelat et al., 2009), gradual down depositional dip variation in the organic matter of the turbidites may be expected. However, as described by Muzzi Magalhaes and Tinterri (2010), the Marnoso-Arenacea basin floor was not entirely flat, nor would one expect any area of the deep-sea to be, and subtle interactions with bathymetry may also have influenced the flow of turbidity currents and their deposits.

Beds associated with the highest density turbidity currents, being those deposited in the lobe axis, have the largest particles and highest proportion of dense organic particles (Fig. 12). As flows passed across the basin, they inevitably lost energy (Kneller, 1995) and their ability to retain large and dense particles in suspension was reduced, giving ever higher proportions of smaller and lighter material through the remaining down-flow depositional elements (Fig. 12). As a consequence, lobe fringe areas show reduced proportions of the densest terrestrial matter and a marked reduction in size, typically being less than half the size of lobe axis particles (Table 3). This is interpreted to represent the deposition of larger, denser particles upstream. Particle size continues to reduce into the fan fringe sub-environment, which sees a marked reduction in sorting (Table 3) as palynomorphs and marine matter became mixed with the terrestrial phytoclasts. Basin plain deposits show a reduction in particle size and less variety of particles. As such it appears the optimum area for the deposition of palynomorphs is in fan fringe or contained interlobe areas.

Contained interlobe deposits may be considered similar to the fan fringe, representing areas of reduced sediment supply; however they show markedly higher proportions of terrestrial material than the fan fringe deposits. This is interpreted as the result of the trapping of suspension clouds, leading to a concentration of terrestrial matter, as opposed to the fan fringe sub-environment, where flows are simply running out from one system and potentially mixing with local marine matter.

A sharp contrast between the palynofacies dominated turbidite elements and the AOM dominated hemipelagic sediments (Fig. 9) can be explained by the difference in sedimentation. Sediments deposited by turbidity currents are rich in terrestrial organic matter supplied from the hinterland and entrained in flows. Hemipelagic sedimentation on the other hand merely represents the fallout of out background marine matter.

The influence of increasing confinement upon the system (Tinterri and Tagliaferri, 2015), particularly the effects of flow stripping, remains to be explored. In theory, this may lead to preferential concentration of denser particles in up-dip areas of a system, however given the studied organic matter is contained within the suspension clouds of turbidity currents, this may actually lead to an increased concentration of organic matter down-dip.

6.3 Comparison with other studies

The palynofacies associations described here can be compared with other documented examples from deep-marine systems. Slope channel-levee systems described by McArthur et al. (2016a) and confined mini-basins described by McArthur et al. (2016b) demonstrated the same types of matter and decay in the density of particles away from sediment conduits (Fig. 13). However the distribution and proportions of organic matter between the various depositional environments presented by each system are markedly different (Fig. 13). Channel-levee systems present much higher ratios of the densest types of matter throughout (McArthur

et al., 2016a), and even the relatively channel distal elements of external levees are unlike the basin floor fan deposits examined here (Fig. 13), despite the sedimentologically similar nature of these thin-bedded elements. The densest fraction of the organic matter, which is abundant in levees, is barley recorded in the Marnoso-Arenacea deposits (Fig. 8).

Although sedimentologically more comparable (Fig. 13), turbidites confined in mini-basins also demonstrate relatively higher proportions of denser particles than observed in the studied basin floor fan (McArthur et al., 2016b). Even the distal thin-bedded elements described are dissimilar, containing much more AOM than the palynofacies dominated thin-beds studied here (Fig. 13). This is likely an effect of the confined nature of the mini-basins, where all the matter becomes trapped and forced out of suspension due to its inability to surmount the basin bounding topography. In the present example, on the contrary, flows were simply grading-out distally without being halted by any flow confinement.

The simplest explanation for the variation in the observed organic particles is the relative distance particles have been transported by turbidity currents. Ricci Lucci (1984) inferred that the Marnoso-Arenacea deposits had already crossed a significant proportion of the basin (at least 60 km) by the observation of more proximal sediments in boreholes drilled to the north. Therefore it is likely that the densest material had already been dropped from flows before they reached the terminal basin floor fan system. This resulted in a concentration of the lightest fraction of the terrestrial matter in the relatively distal reaches of the submarine fan (Fig. 13).

As this represents the third instalment of the attempt to classify turbidite systems with palynofacies, there are not presently other published studies with which to compare our results. We hope this methodology may now be taken up by other workers in order to further test its application across a wider temporal and spatial spectrum.

6.4. Implications for petroleum systems in submarine fan systems

Thin-bed elements are difficult to distinguish sedimentologically or petrophysically, particularly with subsurface data. Although any one sample may not give 100% accuracy in environmental characterisation, several samples over a short interval may provide an interpretation of the depositional environment and should be used in conjunction with other data, such as sedimentological and petrophysical studies to improve interpretations.

This study may have its greatest effect on the analysis of thin-bedded reservoirs, which are becoming ever more important targets for infill drilling (e.g. Weimer et al., 2000). This offers a new tool to distinguish between, fan fringe or contained interlobe, both sedimentologically dominated by mudstone, which may appear similar in wireline or even core studies. However the recognition of contained interlobe deposits may help predict proximity to a nearby lobe with higher reservoir potential.

Although thicker bedded elements, such as the lobe axes are easier to distinguish with traditional methods, the ability to distinguish relatively proximal, often amalgamated from distal, non-amalgamated expressions is clearly of interest to the petroleum geologist. Correct identification of mud-caps (as opposed to clasts), which can present barriers or baffles to flow are essential for obtaining maximum production from a submarine fan reservoir.

That there is an apparent correlation between the thickest, highest reservoir quality sandstones and palynofacies rich in dense terrestrial material may also enable us to link palynofacies with sand proportion. Ideally this may be tested in the subsurface in order to determine if palynofacies is suitable for assisting hydrocarbon exploration and development in deep-marine systems.

7. Conclusions

Depositional environments of a submarine fan system have been analysed from outcrops of the Marnoso-Arenacea Formation, where decades of high resolution documentation of the stratigraphy gives confidence in placement within the system. One hundred and thirty-five samples were collected in conjunction with sedimentary logging in order to examine the palynofacies of submarine fans.

Six lithofacies associations were described, corresponding to depositional environments of the submarine fan system, including lobe axis, lobe fringe, fan fringe, contained interlobe, basin plain, and starved highs. Elements were further subdivided into proximal, intermediate, and distal equivalents based upon sedimentological criteria. Palynological processing and analysis shows the turbidite components to be rich in terrestrial organic matter, with sixteen categories of particulate organic matter observed.

Although all turbidite elements were dominated by palynowafers, the proportions and properties of organic matter show variation between the depositional environments. The proximal lobe axis demonstrates the largest particles and highest proportions of dense matter, such as degraded wood. Down-fan assemblages show a general decrease in dense matter and increasing proportions of lighter material. Intrabasinal highs were starved of sediment, being comprised largely of hemipelagites with their palynofacies being dominated by amorphous organic matter. Therefore the proportions, size, and shape of organic matter can be used to differentiate elements of submarine fans.

Distribution of the organic matter was not random, with hydrodynamic sorting and phased fall-out of matter as turbidity currents ran-out across the basin resulting in different proportions, sizes, and properties of organic matter in sub-environments. This provides a palynofacies classification scheme to assist the identification of depositional environments of basin floor fans. This study provides evidence of the density fractionation of organic matter in

turbidity currents and provides a new way to reconcile the architectural complexity of submarine fans, which can now be applied to subsurface datasets to assist reservoir characterisation.

Acknowledgements

We thank BG Brasil, a wholly owned subsidiary of Royal Dutch Shell plc, for financial support for this project and permission to publish. McArthur is grateful to the Coordenação de Aperfeiçoamento de Pessoal de Nível Superior (CAPES) for the scholarship 049/2012. The Agência Nacional do Petróleo approved this project. Handling and comments by Editor Claudio Nicola Di Celma, as well as constructive reviews by Amandine Prelat and an anonymous reviewer are greatly appreciated.

References cited

- Alpak, F.O., Barton, M.D., and Naruk, S.J., 2013, The impact of fine-scale turbidite channel architecture on deep-water reservoir performance: *AAPG Bulletin*, v. 97, no. 2, p. 251–284.
- Amy, L. A., and Talling, P.J., 2006, Anatomy of turbidites and linked debrites based on long distance (120 x 30 km) bed correlation, Marnoso Arenacea Formation, Northern Apennines, Italy: *Sedimentology*, v. 53, no. 1, p. 161–212, doi: 10.1111/j.1365-3091.2005.00756.x.
- Amy, L.A., Talling, P.J., Sumner, E.J., and Malgesini, G., 2015, Current-aligned dewatering sheets and “enhanced” primary current lineation in turbidite sandstones of the Marnoso-arenacea Formation: *Sedimentology*, v. 63, p. 1260–1279.
- Argnani, A., and Ricci Lucchi, F., 2001, Tertiary silicoclastic turbidite systems of the Northern Apennines, *in Anatomy of an orogen: The Apennines and adjacent Mediterranean basins*, Springer, p. 327–349.
- Barton, M., Byrne, C.O., Pirmez, C., Prather, B., Vlugt, F. Van Der, Alpak, F.O., and Sylvester, Z., 2010, Turbidite Channel Architecture : Recognizing and Quantifying the Distribution of Channel-base Drapes Using Core and Dipmeter Data, *in Poppelreiter, M., García-Carballido, C., and Kraaijveld, M. eds., Dipmeter and borehole image log technology*, p. 195–210.
- di Base, D., and Mutti, E., 2002, The 'Proto Adriatic Basin', *in Mutti, E., Ricci Lucchi, F., and Roveri, M. eds., Revisiting Turbidites of the Marnoso-arenacea Formation and their Basin-Margin Equivalents: Problems with Classic Models. 64th EAGE Conference and Exhibition Excursion Guidebook*, Parma University and ENI-AGIP Division, Parma, Italy, p. I-1-I-4.
- Batten, D.J., 1982, Palynofacies, palaeoenvironments and petroleum: *Journal of Micropalaeontology*, v. 1, no. 1, p. 107–114, doi: 10.1144/jm.1.1.107.
- Baudin, F., Disnar, J.-R., Martinez, P., and Dennielou, B., 2010, Distribution of the organic matter in the channel-levees systems of the Congo mud-rich deep-sea fan (West Africa). Implication for deep offshore petroleum source rocks and global carbon cycle: *Marine*

- and *Petroleum Geology*, v. 27, no. 5, p. 995–1010, doi: 10.1016/j.marpetgeo.2010.02.006.
- Beaudouin, C., Dennielou, B., Melki, T., Guichard, F., Kallel, N., Berné, S., and Huchon, A., 2004, The Late-Quaternary climatic signal recorded in a deep-sea turbiditic levee (Rhône Neofan, Gulf of Lions, NW Mediterranean): palynological constraints: *Sedimentary Geology*, v. 172, no. 1–2, p. 85–97, doi: 10.1016/j.sedgeo.2004.07.008.
- Biscara, L., Mulder, T., Martinez, P., Baudin, F., Etcheber, H., Jouanneau, J.-M., and Garlan, T., 2011, Transport of terrestrial organic matter in the Ogooué deep sea turbidite system (Gabon): *Marine and Petroleum Geology*, v. 28, no. 5, p. 1061–1072, doi: 10.1016/j.marpetgeo.2010.12.002.
- Boulter, M., and Riddick, A., 1986, Classification and analysis of palynodebris from the Palaeocene sediments of the Forties Field: *Sedimentology*, v. 33, no. 4, p. 871–886.
- Bouma, A.H. 1962, Sedimentology of some Flysch deposits: A graphic approach to facies interpretation: PhD thesis, University of Utrecht.
- Bouma, A.H., and Rozman, D.J., 2000, Chapter 25: Characteristics of Fine-Grained Outer Fan Fringe Turbidite Systems, *in* Bouma, A.H. and Stone, C.G. eds., AAPG Memoir 72/SEPM Special Publication No. 68 Fine-Grained Turbidite Systems, AAPG / SEPM, Tulsa, p. 291–298.
- Browne, G.H., and Slatt, R.M., 2002, Outcrop and behind-outcrop characterization of a late Miocene slope fan system, Mt. Messenger Formation, New Zealand: *AAPG Bulletin*, v. 5, no. 5, p. 841–862.
- Caratini, C., 1994, Palynofacies of some recent marine sediments: the role of transportation, *in* Traverse, A. ed., *Sedimentation of Organic Particles*, Cambridge University Press, Cambridge, p. 129–139.
- Caratini, C., Bellet, J., and Tissot, C., 1983, Les palynofaciès: représentation graphique, intérêt de leur étude pour les reconstitutions paléogéographiques, *in* Centre National de la Recherche Scientifique, p. 327–351.
- Cattaneo, A., and Ricci Lucchi, F., 1995, Long-distance correlation of sandy turbidites: a 2.5 km long cross-section of Marnoso-Arenacea, Santerno Valley, Northern Apennines, *in* *Atlas of Deep Water Environments*, Springer, p. 303–306.
- Chaloner, W.G., and Muir, M., 1968, Spores and floras, *in* Murchison, D. and Westoll, T.S. eds., *Coal and coal-bearing strata*, Elsevier, New York, p. 127–146.
- Churchill, J.M., Poole, M.T., Skarpeid, S.S., and Wakefield, M.I., 2016, Stratigraphic architecture of the Knarr Field, Norwegian North Sea: sedimentology and biostratigraphy of an evolving tide- to wave-dominated shoreline system: *Geological Society, London, Special Publications*, v. 444, <http://doi.org/10.1144/SP444.4>
- Combaz, A., 1964, Les palynofaciès: *Revue de Micropaléontologie*, v. 7, p. 205–213.
- Cross, A., Thompson, G., and Zaitzeff, J., 1966, Source and distribution of palynomorphs in bottom sediments, southern part of Gulf of California: *Marine Geology*, v. 4, p. 467–524.
- Dall’Olio, E., Felletti, F., and Muttoni, G., 2013, Magnetic-fabric analysis as a tool to constrain mechanisms of deep-water mudstone deposition in the Marnoso Arenacea Formation (Miocene, Italy): *Journal of Sedimentary Research*, v. 83, no. 2, p. 170–182.

- Daly, R.J., Jolley, D.W., Spicer, R.A., Ahlberg, A., 2011, A palynological study of an extinct arctic ecosystem from the Palaeocene of Northern Alaska: Review of Palaeobotany and Palynology, v. 166, p. 107–116.
- Davey, R.J., 1971, Palynology and palaeo-environmental studies, with special reference to the continental-shelf sediments of South Africa, *in* Farinacci, A. ed., Proceedings of the Second Planktonic Conference, Rome, p. 331–347.
- Davey, R.J., and Rogers, J., 1975, Palynomorph distribution in Recent offshore sediments along two traverses off South West Africa: *Marine Geology*, v. 18, p. 213–225.
- DeVay, J.C., Risch, D. Scott, E. Thomas, C., 2000, A Mississippi-sourced, middle miocene (M4), finegrained abyssal plain fan complex, northeastern Gulf of Mexico, *in* A.H. Bouma and C.G. Stone, eds., Fine-grained turbidite systems, AAPG Memoir 72/SEPM Special Publication 68, p. 109–118.
- Erbs-Hansen, D.R., Knudsen, K.L., Gary, A.C., Gyllencreutz, R., Jansen, E., 2012. Holocene climatic development in Skagerrak, eastern North Atlantic: Foraminiferal and stable isotopic evidence: *The Holocene*, v. 22, p. 301–312.
- Erbs-Hansen, D.R., Knudsen, K.L., Gary, A.C., Jansen, E., Gyllencreutz, R., Scao, V., Lambeck, K., 2011. Late Younger Dryas and early Holocene palaeoenvironments in the Skagerrak, eastern North Atlantic: a multiproxy study: *Boreas*, v. 40, p. 660–680.
- Felletti, F., Dall’Olio, E., and Muttoni, G., 2016, Determining flow directions in turbidites: An integrated sedimentological and magnetic fabric study of the Miocene Marnoso Arenacea Formation (northern Apennines, Italy): *Sedimentary Geology*, v. 335, p. 197–215.
- Gandolfi, G., Paganelli, L., and Zuffa, G.G., 1983, Petrology and dispersal pattern in the Marnoso-arenacea Formation (Miocene, Northern Apennines): *Journal of Sedimentary Research*, v. 53, no. 2, p. 493–507.
- Gary, A.C., Wakefield, M.I., Johnson, G.W., and Ekart, D.D., 2009, Application of Fuzzy C-Means Clustering to Paleoenvironmental Analysis, *in* *Geologic Problem Solving with Microfossils*, SEPM Society for Sedimentary Geology, p. 9–20.
- Houghton, P.D.W., Barker, S.P., and McCaffrey, W.D., 2003, Linked debrites in sand-rich turbidite systems - origin and significance: *Sedimentology*, v. 50, no. 3, p. 459–482, doi: 10.1046/j.1365-3091.2003.00560.x.
- Hempton, M., Marshall, J., Sadler, S., Hogg, N., Charles, R., and Harvey, C., 2005, Turbidite reservoirs of the Sele Formation, Central North Sea: geological challenges for improving production, *in* Geological Society, London, Petroleum Geology Conference series, p. 449–459.
- Heusser, L., 1988, Pollen distribution in marine sediments on the continental margin off northern California: *Marine Geology*, v. 80, p. 131–147.
- Hooghiemstra, H., Lézine, A.-M., Leroy, S. a. G., Dupont, L., and Marret, F., 2006, Late Quaternary palynology in marine sediments: A synthesis of the understanding of pollen distribution patterns in the NW African setting: *Quaternary International*, v. 148, no. 1, p. 29–44, doi: 10.1016/j.quaint.2005.11.005.
- Hoorn, C., 1997, Palynology of the Pleistocene glacial/interglacial cycles of the amazon fan (Holes 940A, 944A and 946A): Proceedings of the Ocean Drilling Program, Scientific

Results, v. 155, p. 397–409.

- Hubbard, S.M., De Ruig, M.J., and Graham, S.A., 2005, Utilizing outcrop analogs to improve subsurface mapping of natural gas-bearing strata in the Puchkirchen Formation, Molasse Basin, Upper Austria: *Austrian Journal of Earth Sciences*, v. 98, p. 52–66.
- Jäger, H., and McLean, D., 2008, Palynofacies and spore assemblage variations of upper Viséan (Mississippian) strata across the southern North Sea: *Review of Palaeobotany and Palynology*, v. 148, no. 2–4, p. 136–153, doi: 10.1016/j.revpalbo.2007.04.005.
- Jobe, Z.R., Bernhardt, A., and Lowe, D.R., 2010, Facies and architectural asymmetry in a conglomerate-rich submarine channel fill, Cerro Toro Formation, Sierra del Toro, Magallanes Basin, Chile: *Journal of Sedimentary Research*, v. 80, no. 12, p. 1085–1108.
- van der Kaars, S., 2001, Pollen distribution in marine sediments from the south-eastern Indonesian waters: *Palaeogeography, Palaeoclimatology, Palaeoecology*, v. 171, no. 3–4, p. 341–361, doi: 10.1016/S0031-0182(01)00253-X.
- Kane, I.A., Pontén, A.S.M., Vangdal, B., Eggenhuisen, J.T., Hodgson, D.M., Sychala, Y.T., 2017, The stratigraphic record and processes of turbidity current transformation across deep-marine lobes: *Sedimentology*, v. 64, p. 1236–1273.
- Kneller, B., 1995, Beyond the turbidite paradigm: physical models for deposition of turbidites and their implications for reservoir prediction: *Geological Society of London Special Publications*, v. 94, p. 31–49. <http://dx.doi.org/10.1144/GSL.SP.1995.094.01.04>.
- Kohl, B., 1985, Biostratigraphy and Sedimentation Rates of the Mississippi Fan, *in* Bouma, A., Normark, W., and Barnes, N. eds., *Submarine Fans and Related Turbidite Systems SE - 39*, *Frontiers in Sedimentary Geology*, Springer New York, p. 267–273.
- Koreneva, E.V., 1971, Spore and pollen in Mediterranean bottom sediments, *in* Funnel, B.M. and Reidel, W.R. eds., *The Micropalaeontology of Oceans*, Cambridge University Press, Cambridge, p. 361–371.
- Lazar, M., Schattner, U., and Reshef, M., 2012, The great escape: An intra-Messinian gas system in the eastern Mediterranean: *Geophysical Research Letters*, v. 39, no. 20, doi: 10.1029/2012GL053484.
- Lucente, C.C., 2004, Topography and palaeogeographic evolution of a middle Miocene foredeep basin plain (Northern Apennines, Italy): *Sedimentary Geology*, v. 170, no. 3, p. 107–134.
- Lucente, C.C., and Pini, G.A., 2008, Basin-wide mass-wasting complexes as markers of the Oligo-Miocene foredeep-accretionary wedge evolution in the northern Apennines, Italy: *Basin Research*, v. 20, no. 1, p. 49–71.
- Malgesini, G., Talling, P.J., Hogg, A.J., Armitage, D., Goater, A., and Felletti, F., 2015, Quantitative analysis of submarine-flow deposit shape in the Marnoso-Arenacea Formation: what is the signature of hindered settling from dense near-bed layers? *Journal of Sedimentary Research*, v. 85, no. 2, p. 170–191.
- Martin, M.A., Wakefield, M., MacPhail, M.K., Pearce, T., and Edwards, H.E., 2013, Sedimentology and stratigraphy of an intra-cratonic basin coal seam gas play: Walloon Subgroup of the Surat Basin, eastern Australia: *Petroleum Geoscience*, v. 19, no. 1, p. 21–38.
- McArthur, A.D., Kneller, B.C., Souza, P.A., and Kuchle, J., 2016a, Characterization of deep-

- marine channel-levee complex architecture with palynofacies: an outcrop example from the Rosario Formation, Baja California, Mexico: *Marine and Petroleum Geology*, v. 73, p. 157–173, doi: 10.1016/j.marpetgeo.2016.02.030.
- McArthur, A.D., Kneller, B.C., Wakefield, M.I., Souza, P.A., and Kuchle, J., 2016b, Palynofacies classification of the depositional elements of confined turbidite systems: Examples from the Gres d'Annot, SE France: *Marine and Petroleum Geology*, v. 77, p. 1254–1273.
- Mulder, T., Etienne, S., 2010, Lobes in deep-sea turbidite systems: State of the art: *Sedimentary Geology*, v. 229, p. 75-80.
- Muller, J., 1959, Palynology of Recent Orinoco delta and shelf sediments: Reports of the Orinoco Shelf Expedition; Volume 5: Micropaleontology, v. 5, no. 1, p. 1–32.
- Mutti, E., Ricci Lucchi, F., and Roveri, M., 2002, Revisiting Turbidites of the Marnoso-arenacea Formation and their Basin-Margin Equivalents: Problems with Classic Models. 64th EAGE Conference and Exhibition Excursion Guidebook: Parma University and ENI-AGIP Division, Parma, Italy.
- Mutti, E., Tinterri, R., Benevelli, G., di Biase, D., and Cavanna, G., 2003, Deltaic, mixed and turbidite sedimentation of ancient foreland basins: *Marine and Petroleum Geology*, v. 20, no. 6, p. 733–755.
- Muzzi Magalhaes, P., and Tinterri, R., 2010, Stratigraphy and depositional setting of slurry and contained (reflected) beds in the Marnoso-arenacea Formation (Langhian-Serravallian) Northern Apennines, Italy: *Sedimentology*, v. 57, no. 7, p. 1685–1720.
- Neavel, R.C., 1981, Origin, petrography, and classification of coal, *in* Elliott, M.A. ed., *Chemistry of Coal Utilization*, Wiley, New York, p. 91–158.
- Oboh-Ikuenobe, F., and Yepes, O., 1997, Palynofacies analysis of sediments from the Côte d'Ivoire-Ghana transform margin: Preliminary correlation with some regional events in the Equatorial Atlantic: *Palaeogeography, Palaeoclimatology, Palaeoecology*, v. 129, p. 291–314.
- Oboh-Ikuenobe, F.E., Hoffmeister, A.P., and Chrisfield, R.A., 1999, Cyclical distribution of dispersed organic matter and dinocysts, ODP site 959 (early Oligocene-early Miocene, Côte d' Ivoire-Ghana transform margin): *Palynology*, v. 23, p. 87–96.
- Oyedele, O.A., Dupré, W.R., and Marfurt, K.J., 2015, Seismic Facies Analysis and Age Dating of Mid-Pleistocene Channel-Lobe Deposits, Mad Dog Field, Gulf of Mexico: *Gulf Coast Association of Geological Societies Transactions*, v. 65, p. 301–312.
- Parry, C., Whitley, P.K.J., and Simpson, R.D.H., 1981, Integration of palynological and sedimentological methods in facies of the Brent Formation, *in* Illing, L.V. and Hobson, G.D. eds., *Petroleum Geology of the Continental Shelf of North-West Europe*, Heyden, London, p. 205–215.
- Patacci, M., Houghton, P.D.W., McCaffrey, W.D., 2015, Flow Behavior of Pondered Turbidity Currents: *Journal of Sedimentary Research*, v. 85, p. 885-902; DOI: 10.2110/jsr.2015.59
- Prelat, A., Hodgson, D.M., and Flint, S.S., 2009, Evolution, architecture and hierarchy of distributary deep-water deposits: a high-resolution outcrop investigation from the Permian Karoo Basin, South Africa: *Sedimentology*, v. 56, no. 7, p. 2132–2154, doi: 10.1111/j.1365-3091.2009.01073.x.

- Reading, H., and Richards, M., 1994, Turbidite systems in deep-water basin margins classified by grain size and feeder system: AAPG bulletin, v. 78, p. 792–822.
- Ricci Lucchi, F., 1965, Alcune strutture di risedimentazione nella formazione marnoso-arenacea romagnola: *Giornale di Geologia*, v. 33, no. 2, p. 265–292.
- Ricci Lucchi, F., 1967, Recherches stratonomiques et sedimentologiques sur le flysch Miocene de la Romagna: *Giornale di Geologia*, v. 35, p. 163–192.
- Ricci Lucchi, F., 1969, Channelized deposits in the middle Miocene flysch of Romagna (Italy): *Giornale di Geologia*, v. 36, p. 203–282.
- Ricci Lucchi, F., 1975a, Depositional Cycles in Two Turbidite Formations of Northern Apennines (Italy): *Journal of Sedimentary Petrology*, v. 45, no. 1, p. 3–43.
- Ricci Lucchi, F., 1975b, Miocene paleogeography and basin analysis in the Periadriatic Apennines: *Petroleum Exploration Society of Libya*.
- Ricci Lucchi, F., 1978, Turbidite dispersal in a Miocene deep-sea plain: the Marnoso-arenacea of the northern Apennines: *Geologie en Mijnbouw*, v. 57, no. 4, p. 559–576.
- Ricci Lucchi, F., 1983, The deep-sea fan deposits of the Miocene Marnoso-Arenacea Formation, northern Apennines: *Geo-marine letters*, v. 3, no. 2–4, p. 203–210.
- Ricci Lucchi, F., 1985, Marnoso-arenacea turbidite system, Italy, *in* *Submarine Fans and Related Turbidite Systems*, Springer, p. 209–216.
- Ricci Lucchi, F., 1986, The Oligocene to Recent foreland basins of the northern Apennines, *in* Allen, P. a. and Homewood, P. eds., *Foreland basins*, Blackwell Scientific, p. 103–139.
- Ricci Lucchi, F., 1995, Contessa and associated megaturbidites: long distance (120\times 25 km) correlation of individual beds in a Miocene foredeep, *in* Pickering, K.T., Hiscott, R., Kenyon, N.H., Ricci Lucchi, F., and Smith, R.D.. eds., *Atlas of Deep Water Environments*, Chapman & Hall, London, p. 300–302.
- Ricci Lucchi, F., and Valmori, E., 1980, Basin-wide turbidites in a Miocene, over-supplied deep-sea plain: a geometrical analysis: *Sedimentology*, v. 27, no. 3, p. 241–270.
- Riley, G.A., 1970, Particulate organic matter in seawater: *Advances in Marine Biology*, v. 8, p. 1–118.
- Rose, P., Pyle, J., Barker, G., Koster, K., and others, 2011, Forties infill drilling eight years on; continued success through the application of thorough development geoscience driven by 4D seismic, *in* *Offshore Europe*, Society of Petroleum Engineers.
- Roveri, M., Ricci Lucchi, F., Lucente, C.C., Manzi, V., Mutti, E., 2002, Stratigraphy, facies and basin fill history of the Marnoso-arenacea Formation, *in* Mutti, E., Ricci Lucchi, F., and Roveri, M. eds., *Revisiting turbidites of the Marnoso-arenacea Formation and their basin-margin equivalents: problems with classic models*. 64th EAGE Conference and Exhibition. Excursion Guidebook, Parma University and ENI-AGIP Division, Parma, Italy, p. III-1-III-26.
- Schiøler, P., Rogers, K., Sykes, R., Hollis, C.J., Ilg, B., Meadows, D., Roncaglia, L., and Uruski, C., 2010, Palynofacies, organic geochemistry and depositional environment of the Tartan Formation (Late Paleocene), a potential source rock in the Great South Basin, New Zealand: *Marine and Petroleum Geology*, v. 27, no. 2, p. 351–369, doi:

10.1016/j.marpetgeo.2009.09.006.

- Shepard, F.P., 1956, Marginal sediments of Mississippi delta: AAPG Bulletin, v. 40, no. 11, p. 2537–2623.
- Spicer, R.A., 1989, The formation and interpretation of plant fossil assemblages: *Advances in Botanical Research*, v. 16, p. 95-191.
- Stanley, D.J., 1986, Turbidity current transport of organic-rich sediments: Alpine and Mediterranean examples: *Marine Geology*, v. 70, no. 1–2, p. 85–101, doi: 10.1016/0025-3227(86)90090-3.
- Staplin, F.L., 1969, Sedimentary organic matter, organic metamorphism, and oil and gas occurrence: *Bulletin of Canadian Petroleum Geology*, v. 17, no. 1, p. 47–66.
- Stetten, E., Baudin, F., Reyss, J.-L., Martinez, P., Charlier, K., Schnyder, J., Rabouille, C., Dennielou, B., Coston-Guarini, J., and Pruski, A., 2015, Organic matter characterization and distribution in sediments of the terminal lobes of the Congo deep-sea fan: Evidence for the direct influence of the Congo River: *Marine Geology*, v. 369, p. 182–195.
- Sumner, E.J., Talling, P.J., Amy, L. a., Wynn, R.B., Stevenson, C.J., and Frenz, M., 2012, Facies architecture of individual basin-plain turbidites: Comparison with existing models and implications for flow processes: *Sedimentology*, v. 59, no. 6, p. 1850–1887, doi: 10.1111/j.1365-3091.2012.01329.x.
- Tagliaferri, A and Tinterri, R., 2016, The tectonically confined Firenzuola turbidite system (Marnoso-arenacea Formation, northern Apennines, Italy): *Italian Journal of Geosciences*, v. 135, p. 425-443, doi: 10.3301/IJG.2015.27
- Talling, P.J., 2001, On the frequency distribution of turbidite thickness: *Sedimentology*, v. 48, p. 1297-1329.
- Talling, P.J., Amy, L. A., Wynn, R.B., Blackbourn, G., and Gibson, O., 2007, Evolution of Turbidity Currents Deduced from Extensive Thin Turbidites: Marnoso Arenacea Formation (Miocene), Italian Apennines: *Journal of Sedimentary Research*, v. 77, no. 3, p. 172–196, doi: 10.2110/jsr.2007.018.
- Talling, P.J., Malgesini, G., Sumner, E.J., Amy, L.A., Felletti, F., Blackbourn, G., Nutt, C., Wilcox, C., Harding, I.C., and Akbari, S., 2012, Planform geometry, stacking pattern, and extrabasinal origin of low strength and intermediate strength cohesive debris flow deposits in the Marnoso-arenacea Formation, Italy: *Geosphere*, GES00734--1.
- Talling, P.J., Malgesini, G., and Felletti, F., 2013, Can liquefied debris flows deposit clean sand over large areas of sea floor? Field evidence from the Marnoso-arenacea Formation, Italian Apennines: *Sedimentology*, v. 60, no. 3, p. 720–762.
- Tinterri, R., and Muzzi Magalhaes, P., 2011, Synsedimentary structural control on foredeep turbidites: An example from Miocene Marnoso-arenacea Formation, Northern Apennines, Italy: *Marine and Petroleum Geology*, v. 28, no. 3, p. 629–657, doi: 10.1016/j.marpetgeo.2010.07.007.
- Tinterri, R., and Tagliaferri, A., 2015, The syntectonic evolution of foredeep turbidites related to basin segmentation: Facies response to the increase in tectonic confinement (Marnoso-arenacea Formation, Miocene, Northern Apennines, Italy): *Marine and Petroleum Geology*, v. 67, p. 81–110.
- Tinterri, R., Muzzi Magalhaes, P., Tagliaferri, A., and Cunha, R.S., 2016, Convolute

- laminations and load structures in turbidites as indicators of flow reflections and decelerations against bounding slopes. Examples from the Marnoso-arenacea Formation (northern Italy) and Annot Sandstones (south eastern France): *Sedimentary Geology*, v. 344, p. 382-407.
- Traverse, A., and Ginsburg, R., 1967, Pollen and associated microfossils in the marine surface sediments of the Great Bahama Bank: *Review of Palaeobotany and Palynology*, v. 3, no. 1967, p. 243–254.
- Tyson, R. V., 1984, Palynofacies investigation of Callovian (Middle Jurassic) sediments from DSDP Site 534, Blake-Bahama Basin, Western Central Atlantic: *Marine and Petroleum Geology*, v. 1, no. 1, p. 3–13, doi: 10.1016/0264-8172(84)90116-8.
- Tyson, R. V., 1995, *Sedimentary Organic Matter*: Chapman & Hall, London.
- Uchupi, E., and Jones, G.F., 1967, Woody debris on the mainland shelf off Ventura, southern California: *Sedimentology*, v. 8, no. 2, p. 147–151.
- Weimer, P., Slatt, R.M., Dromgoole, P., Bowman, M., and Leonard, A., 2000, Developing and managing turbidite reservoirs: case histories and experiences: results of the 1998 EAGE/AAPG Research Conference: *AAPG bulletin*, v. 84, no. 4, p. 453–465.
- Whitaker, M.F., Giles, M.R., and Cannon, S.J.C., 1992, Palynological review of the Brent Group, UK sector, north sea: *Geological Society, London, Special Publications*, v. 61, no. 1, p. 169–202, doi: 10.1144/GSL.SP.1992.061.01.10.
- Wickens, Hd., and Bouma, A.H., 2000, The Tanqua fan complex, Karoo Basin, South Africa-outcrop analog for fine-grained, deepwater deposits: *SPECIAL PUBLICATION-SEPM*, v. 68, p. 153–164.
- Zadeh, L.A., 1965, Fuzzy Sets: *Information and control*, v. 8, p. 338–353.
- van der Zwan, C.J., 1990, Palynostratigraphy and Palynofacies Reconstruction of the Upper Jurassic to Lowermost Cretaceous of the: *Review of Palaeobotany and Palynology*, v. 62, p. 157–186.
- Zonneveld, K.A.F., Versteegh, G.J.M., Kasten, S., Eglinton, T.I., Emeis, K.-C., Huguet, C., Koch, B.P., de Lange, G.J., De Leeuw, J.W., Middelburg, J.J., Mollenhauer, G., Prahl, F.G., Rethemeyer, J., and Wakeham, S.G., 2010, Selective preservation of organic matter in marine environments; processes and impact on the sedimentary record: *Biogeosciences*, v.7, p. 483-511.

Figure captions

Fig. 1. A) Structural map of the northern Apennines (modified from Tinterri and Magalhaes 2011), showing studied sections. Inset Google Earth image of Italy. B) Generalised stratigraphic column for the studied portion of the Marnoso-Arenacea Formation, modified from Tinterri and Magalhaes (2011).

Fig. 2. Particulate organic matter encountered in this study, arranged by inferred density. Description based upon our observations and hydrodynamic properties based upon characteristics documented by previous workers. All scale bars 50 μ m.

Fig. 3. Example log and illustrative photo through a proximal lobe (sub-environment A) grading to lobe fringe (sub-environment B) deposits at Firenzuola.

Fig. 4. Example log and illustrative photo through distal fan fringe deposits (sub-environment C) at Cabelli. Note the colour difference between lower, dark grey mudstone of turbidite facies F4 and upper, light grey hemipelagic mudstones (F5). Key to log as with figure 3.

Fig. 5. Example log and illustrative photo through interlobe deposits (sub-environment D) at Firenzuola. Key to log as with figure 3.

Fig. 6. Example log and illustrative photo through basin plain deposits (sub-environment E) at Mandrioli. Pole in photo is 2 m tall. Key to log as with figure 3.

Fig. 7. Example log and illustrative photo through condensed deposits (sub-environment F) at Verghereto. Key to log as with figure 3.

Fig. 8. Count data for each sample organised by depositional environment and in stratigraphic order; Eq – equant opaque debris; DM – dark structureless organic matter; R – resin; Blade – bladed opaque debris; FA – freshwater algae; Z – zoomorphs; A – acritarchs; BS – bisaccate pollen; MA – marine algae.

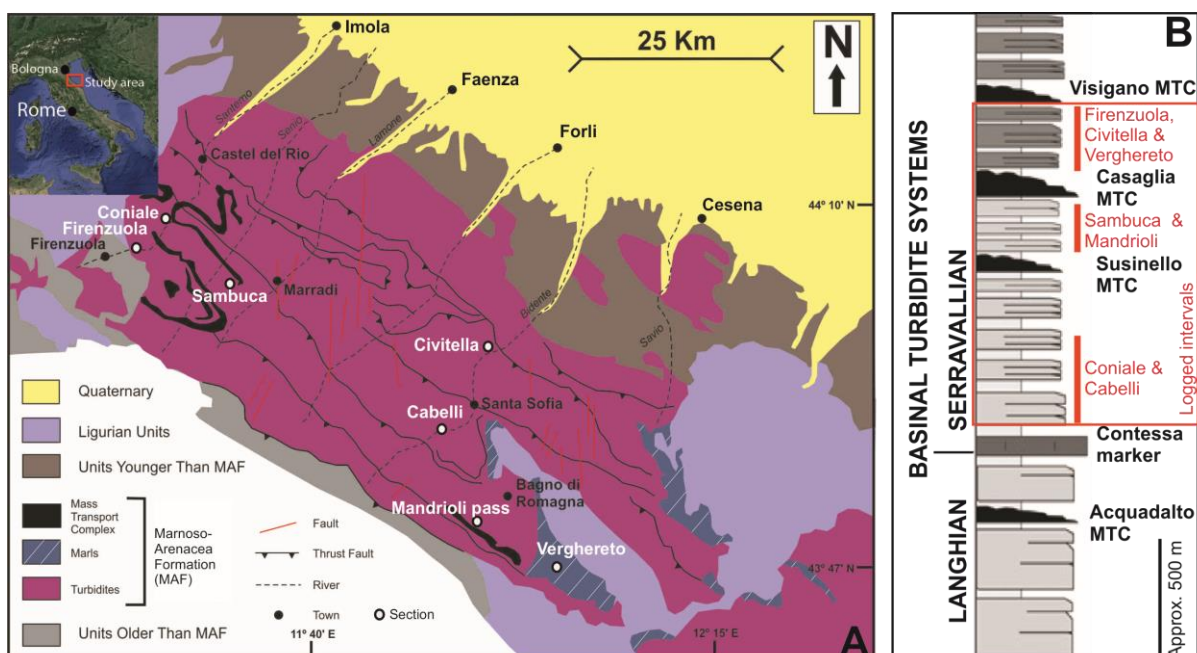
Fig. 9. Box and whisker charts of the proportions of particulate organic matter recorded for each sample from the studied depositional environments; DSOM – dark structureless organic matter; Degrade – degraded wood; FWA – freshwater algae; Sacs – bisaccate pollen; Zoo – zoomorphs; MA – marine algae; AOM – amorphous organic matter. Boxes represent the 25th to 75th percentile, whiskers represent the 25th percentile minus 1.5 times the range of the box and the 75th percentile plus 1.5 times the range of the box values (interquartile range).




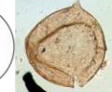



























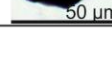
Fig. 10. Representative photomicrographs of A) proximal lobe axis, with large fragments of degraded brown wood; B) intermediate lobe axis, dominated by palynofaers; C) proximal lobe fringe, with palynofaers and degraded wood; D) intermediate lobe fringe, dominated by palynofaers, with degraded and well preserved wood; E) distal lobe fringe, dominated by bacterially degraded palynofaers; F) proximal fan fringe, with palynofaers, amorphous organic matter (AOM) and palynomorphs; G) intermediate fan fringe, H) distal fan fringe, dominated by palynofaers, with degraded wood and AOM I) contained interlobe, very rich in palynofaers, with bladed opaque debris; and J) basin plain architectural elements palynofacies, with AOM and dinocysts. All at same scale.

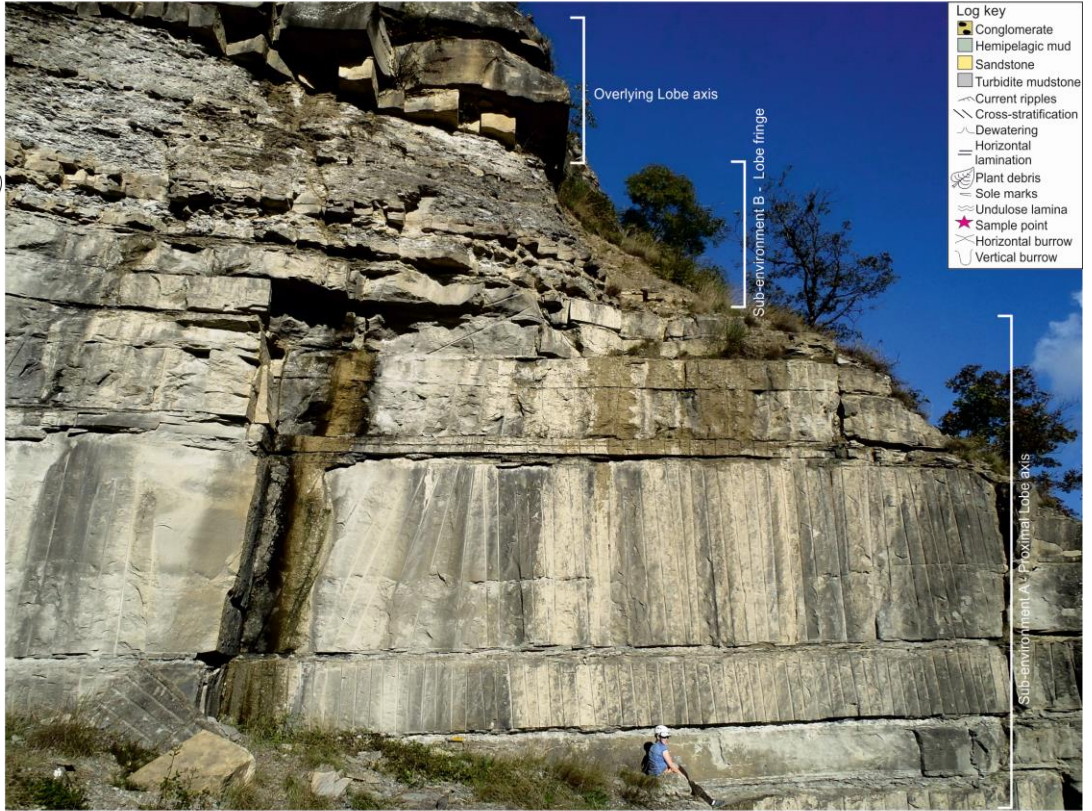
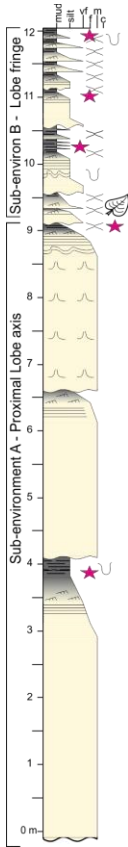
Fig. 11. Fuzzy-cluster (FCM) analysis plots of the Marnoso-Arenacea dataset. The membership of each sample to each cluster is plotted. BP – basin plain; DFF – distal fan fringe; MFF – intermediate fan fringe; PFF – proximal fan fringe; DI – distal contained interlobe; MI – intermediate contained interlobe; PI – proximal contained interlobe; ML – intermediate lobe axis; PL – proximal lobe axis; DLF – distal lobe fringe; MLF – intermediate lobe fringe; PLF – proximal lobe fringe.

Fig. 12. Schematic illustration of the distribution of particulate organic matter in a basin floor fan system. As turbidity currents passed down-stream their ability to maintain larger, denser particles in suspension may be diminished.

Fig. 13. Schematic distribution of particulate organic matter in deep-marine systems, from slope channels (modified from McArthur et al., 2016a), confined mini-basins (modified from McArthur et al., 2016b), and basin floor fans (this study). Figure inspired by DeVey and others (2000).

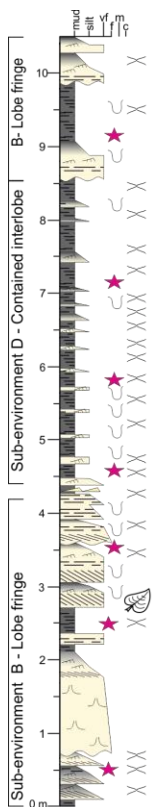
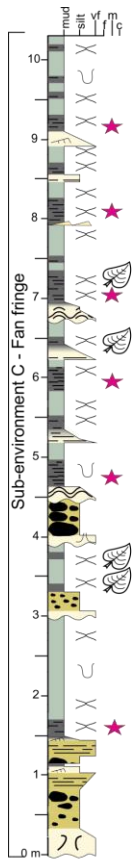


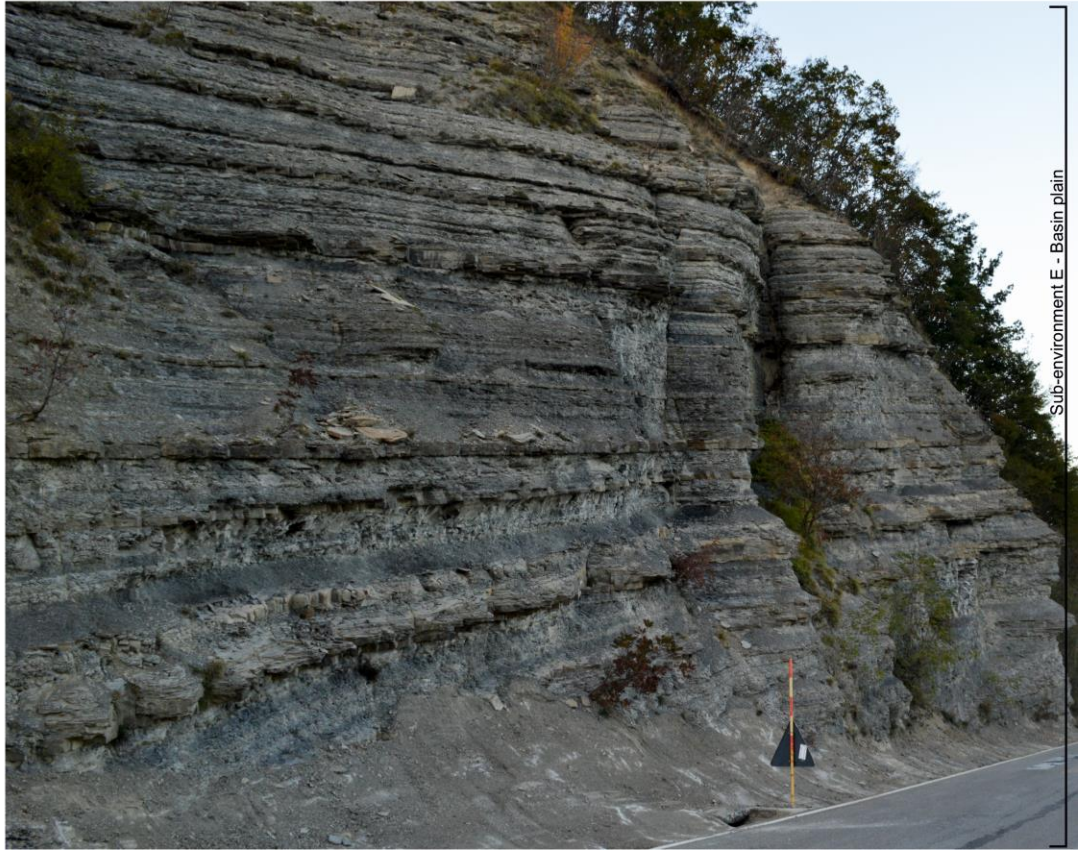
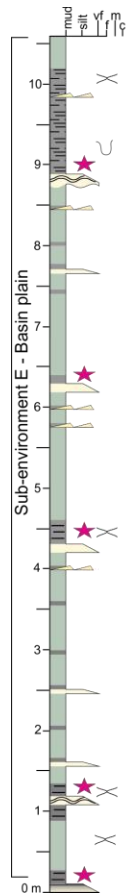
	Particulate organic matter	Description	Hydrodynamic properties			
light ↑	Amorphous group	AMORPHOUS ORGANIC MATTER (sapropel / specs) - marine	Dark brown to transparent, weakly fluorescent, structureless with diffuse edges, often with inclusions, sheet like. Occur as globular "specks" <5 µm and larger (<100 µm) mats.	Represent plankton faecal pellets and larger bacterially degraded mats. Abundant in marine settings, may be truly autochthonous, (Tyson, 1995), but can be transported.		
		MARINE ALGAE - marine	Prasinophyte marine algae, including small leiospheres (<10 µm) and larger forms such as tasmanitids (>50 µm).	Very buoyant pelagic organisms. Typically found in open marine environments and may represent truly autochthonous material in the deep-marine (Kohl 1985).		
		SACCATE POLLEN GRAINS - terrestrial	Saccate pollen, <70 µm, separated from miospores due to their capacity for transportation (Chaloner & Muir, 1968).	Assisted by buoyancy sacs may travel 1000's of km in air and water (Muller 1959).		
Sorted by inferred density ↑	Palyomorph group	ACRITARCHS - marine	Small (<20 µm) thorny forms. Transport is inferred, being predominantly shallow water.	Small planktonic habit aids buoyancy (Tyson, 1995). Processes assist auto-suspension.		
		DINOFLLAGELLATE CYSTS - marine	Composed of dinosporin, 20-100 µm long, dinocysts demonstrate many forms with subsequent effects on transport (Tyson, 1995).	May be in-situ but transport is inferred. Dinocysts are considered to have similar density to fine silt - clay particles, but are denser than saccate pollen (Tyson, 1995).		
		ZOOMORPHS (foraminiferal test linings) - marine	Acid resistant, organic coating of foraminifera chambers. Additional types of zoomorphs were not observed.	Benthic forms may be in-situ, but heavier than marine algae and not be so easily transported (Tyson, 1995).		
		FRESHWATER ALGAE (e.g. Botryococcus)	Orange to brown, colonial algae occurs as clusters <100 µm. Similar properties to DSOM but shows fluorescence.	Designed for buoyancy, though large mats must be considered less buoyant than singular marine algae (Tyson, 1995).		
		FUNGAL SPORES AND HYPHAE - mixed origin	Dark brown, consisting of broken hyphae, fruiting bodies < 100 µm and small, spherical spores <20 µm.	Similar density to miospores, but can be transported further due to their shape and size (Hoorn, 1997).		
dense ↓	Phytoclast group	MIOSPORES - terrestrial	Spores and non-saccate pollen. Exhibit variability in size, thickness and ornament, typically small (<25 µm), smooth, simple forms.	Optimized for dispersion, considered buoyant and are equivalent to silt grade sediment (Muller, 1959).		
		PALYNOWAFERS - mixed origin	Pale brown to transparent, non-fluorescing, thin, irregularly shaped, <300 µm. Includes leaf cuticle and aqueous plant fragments.	The lightest type of phytoclast, platy habit inhibits settling and is readily dispersed (Boulter & Riddick, 1986).		
		BLADED OPAQUE DEBRIS - terrestrial	Similar properties to equant opaque debris, except length is >3 x the width.	Resistant to degeneration and shape assists transport (Van der Zwan, 1990).		
		RESIN - terrestrial	Orange, lustrous, fluorescent, typically spherical and conchoidal, <50 µm.	Similar density to wood, often concentrated in low energy settings (Tyson, 1995).		
		WELL PRESERVED WOOD & PARENCHYMA	Dark brown to yellow, non-fluorescent, structured, lath shaped, <100 µm. Parenchyma and wood demonstrating clear structure, e.g. xylem tracheids and pits.	Structure reduces weight and improves buoyancy (Boulter & Riddick, 1986), thus can be retained in suspension longer than degraded wood.		
		DEGRADED BROWN WOOD - terrestrial origin	Dark brown to yellow, non-fluorescent, unstructured wood fragments, typically flat, <200 µm. Does not exhibit structures, but is completely degraded, retaining cell forms	Typically smaller and thinner than DSOM, and often lath shaped. Thus is relatively lighter than DSOM (Whitaker et al., 1992).		
		DARK STRUCTURELESS ORGANIC MATTER (DSOM) - terrestrial	Dark brown to orange, non-fluorescent, structureless, defined edges, <300 µm. Includes heavily degraded plant debris, humic gels, and resinous cortex.	Large size and spongy nature indicate a low buoyancy (Whitaker et al., 1992). It is susceptible to waterlogging and destruction during transport (Whitaker et al., 1992).		
	EQUANT OPAQUE DEBRIS - oxidised wood of terrestrial origin	Opaque, equidimensional, non-fluorescent, <200 µm in diameter. Angular to well-rounded, may show a smooth or degraded surface. Doesn't include minerals e.g. pyrite.	Heaviest and most resistant to degradation, principally comprised of inertinite. Oxidised plant tissue often concentrated in high energy environments (Whitaker et al., 1992).			



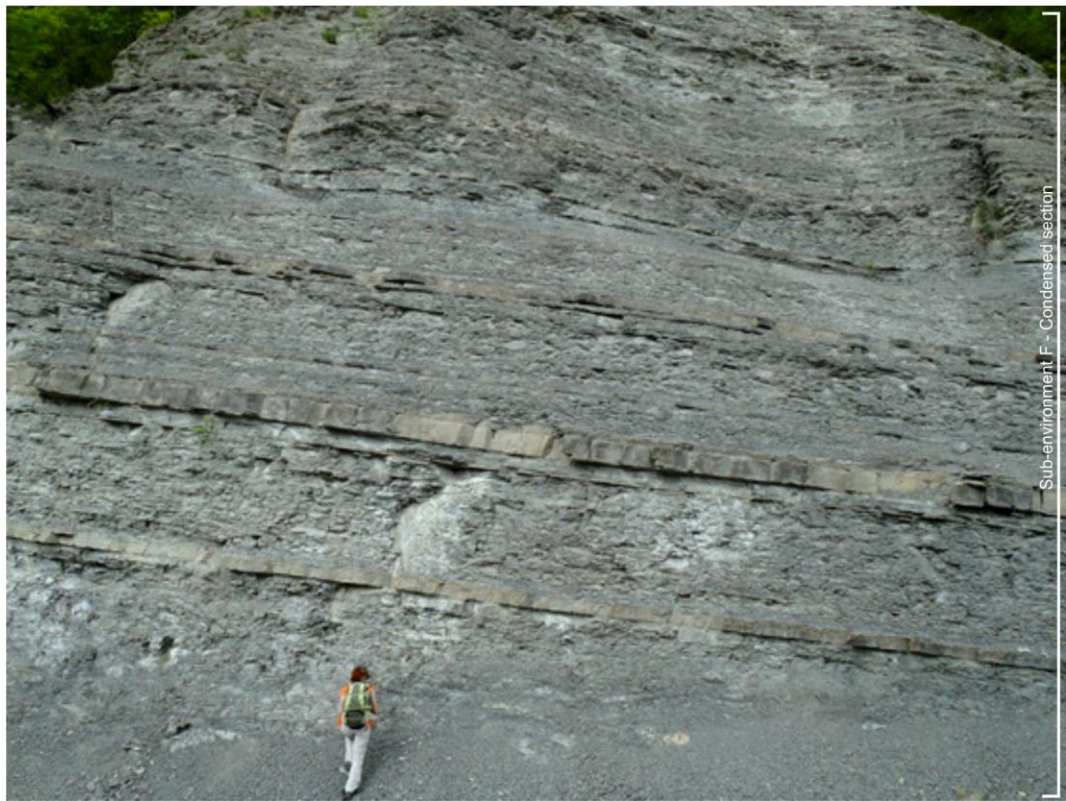
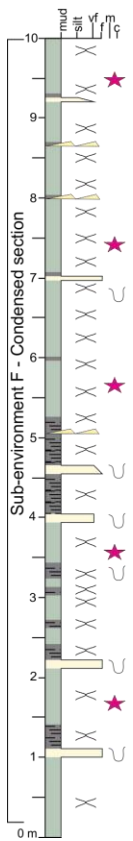
Log key

- Conglomerate
- Hemipelagic mud
- Sandstone
- Turbidite mudstone
- Current ripples
- Cross-stratification
- Dewatering
- Horizontal lamination
- Plant debris
- Sole marks
- Undulose lamina
- Sample point
- Horizontal burrow
- Vertical burrow





Sub-environment E - Basin plain



Sub-environment F - Condensed section

